Power Consumption Considerations for Ultrasound Capsule Endoscopy

Alexandru C. Moldovan[1] , Bartas Abaravičius[2], Srinjoy Mitra[2], Sandy Cochran[1]
[1]James Watt School of Engineering, University of Glasgow, Glasgow, UK
[2]Scottish Microelectronics Center, the University of Edinburgh, Edinburgh, UK
alexandru.moldovan@glasgow.ac.uk

***Abstract*— Ultrasound capsule endoscopy (USCE) promises to combine the usefulness of the traditional endoscope with the increased comfort, reduced risks, and wider reach of a capsule for diagnosis of gastrointestinal tract (GIT) diseases. Equipped with a microultrasound (µUS) array operating at frequencies higher than 20 MHz, the USCE device can benefit from increased axial resolution, while the use of an array can provide a wider field of view via electronic beam-steering. However, reduced available power and limited physical dimensions are obstacles presently hindering the development of such medical devices. This paper proposes and evaluates US array driving techniques to reduce power consumption, discusses the limitations of receiving electronics and considers achievable B-mode imaging frame rates. Two array drivers were used in this study: a custom-made CMOS pulser, with details published previously, and a commercial research array controller (Vantage HF 128, Verasonics, WA, USA). Peak (i_{peak}) and average (i_{avg}) supply current measurements performed for a variable number of elements transmitting (Tx) simultaneously in a 28 MHz µUS array (Vermon, France) show that Tx apertures comprising <7 active elements are most suitable. Furthermore, because of the high i_{peak} supplied to the array, charge storage on board the USCE device is required for any Tx configuration.**

Keywords*— *Ultrasound capsule endoscopy, microultrasound, ultrasonic array, power consumption, ingestible electronics

I. Background and Motivation

Diagnosis and monitoring of GIT diseases is conventionally performed with a tethered endoscope which comprises a camera for optical imaging of the gut mucosa, an ultrasonic (US) probe for differentiating between tissue layers via sonography, or a combination of the two sensors for enhanced scanning [1]. Because of the semi-rigid construction of the endoscope, the procedure is often painful and thus requires sedation, carries the risk of tissue perforation and must be performed by a highly-trained clinician [1]. Furthermore, the reach of the endoscope is limited and it cannot readily be used for diagnosis in deeper parts of the GIT, such as the small bowel.

Ultrasound capsule endoscopy (USCE, Fig. 1.) is a promising approach to overcome most of the shortcomings of the conventional approach by incorporating the relevant sensors into a less invasive, ingestible capsule. This can reach the entire GIT via natural locomotion and also offers the prospect of remote positioning at a desired location via magnetically-coupled robotic manipulation [3].

Video capsule endoscopy (VCE) has been in clinical use since 2001 [4]; however, implementation of US imaging transducers into ingestible capsules has not yet been achieved commercially because of the size and complexity of the electronic components. Capsules equipped with stationary single element transducers have limited field of view and require complex positioning mechanisms to scan the circumference of the bowel. Several capsules using transducers rotated by a motor have been successfully demonstrated in-vivo [1], [2], [5], [6] and these are capable of providing circumferential US scans of the GIT. However, the motor is bulky, requires large driving currents and is not compatible with magnetic manipulation.

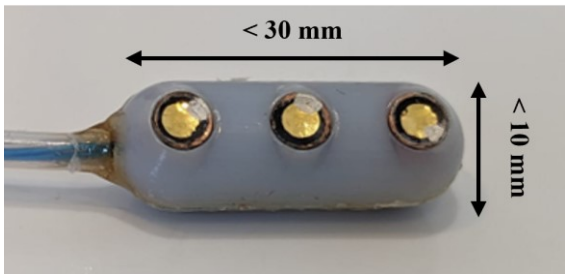

Fig. 1. Photograph of a tethered USCE device prototype depicting its maximum dimensions

The use of an US array can replace the motor assembly with electronic beam-steering and focusing. However, miniaturisation of multi-channel electronics and the limited power on-board the capsule have so far hindered the successful development of a wireless USCE device equipped with a µUS array. Taking into account advances in wireless power transfer systems and silicon chip manufacturing capabilities that allow close incorporation of the control electronics and the transducers [7], we are exploring the feasibility of a tetherless microultrasound capsule endoscopy (µUSCE) device; here, we focus on power consumption specifically.

II. Aim of Study

The electrical power supply available to capsule electronics from an in-built battery or a wireless receiver is limited to around 300 mW in air, in laboratory conditions [8], which is shared between the US transmission (Tx) and reception (Rx) circuits.

In this paper we evaluate array driving procedures that minimize power consumption during US transmission for USCE by measuring the peak (i_{peak}) and the average current (i_{avg}) required for different Tx partial aperture sizes. The transducer used for the measurements was a 128 element, 28 MHz µUS array (Vermon, France), operating at a frequency suitable for differentiating between the gut tissue layers.

Furthermore, we discuss the limitations of the Rx aperture size in relation to the available electronics and evaluate the imaging frame rate that is achievable with the proposed data acquisition settings. These results will potentially serve as guidelines for the design of custom-made CMOS electronics for USCE implementation.

This work was carried out as part of the AUTOCAPSULE project funded by the European Union's Horizon 2020 Research and Innovation Programme under grant agreement no. 952118.

III. Technical Background

A. Power Consumption and Space Considerations for USCE

Commercial VCE devices rely on two coin-cell batteries as the energy source and have been shown to have power consumption of around 20 mW [9], which allows them to operate for up to 12 hours on the available battery charge. However, a µUS transducer and its associated electronics have significantly higher power consumption than the video sensor, thus requiring a larger supply. Wireless power transfer (WPT) can potentially solve this problem by delivering constant power from outside the patient's body using an inductive link. Considering specific absorption rate (SAR) limitations for human use, WPT was demonstrated to deliver up to 75 mW to a capsule endoscope placed inside a muscle tissue phantom [10].

For acoustic transmission, US imaging systems based on commercial off-the-shelf (COTS) components commonly use a single high-voltage (HV) pulse generator circuit and subsequently multiplex the signal to the required array elements using an analogue multiplexer. The pulser circuit comprises multiple components which, together with the multiplexer, lead to significant system silicon area overhead. Additionally, parasitic capacitances within the components and interconnects increase power consumption. One of the most recent examples, by Lin et al. [11], demonstrated a COTS-based US system for health monitoring using a 32-element array. It required ~614 mW average power and had a footprint of 21 cm^2, both values too high for USCE.

For the reception of µUS data from multiple array elements, fast analogue-to-digital converters (ADCs) are a requirement which, in turn, leads to high power drain by the Rx electronics. For transducers operating above 20 MHz, the sampling frequency must be ~125 Msps. Presently, commercial, low power, high-frequency ADCs with the required bandwidth consume ~100 mW per channel, which is a limiting factor for the number of parallel receive channels available in an USCE device. Lower power implementations have been published in literature but they are yet to be verified in US applications [12].

A subsequent design challenge of an USCE system is the fluctuation in the instantaneous power required. During the US Tx phase, the highest demand comes from the HV generation circuit responsible for driving the array elements, while, during US Rx, the power consumption is split between the low-voltage analogue front-end (AFE), the ADC, and the microcontroller. A block diagram of the electronics for an USCE device is presented in Fig. 2. During the US Tx and Rx phases (i.e. the active phases), the power drawn from the battery/WPT can be hundreds of mW, exceeding the instantaneous capacity of the energy source. Considering that the imaging frame rate for USCE is low (~1 - 10 Hz), corresponding to a duty cycle between ~0.1% and 1%, the inactive phase could be used for data transfer, while keeping the capsule electronics in a low-power mode. Furthermore, by including local energy storage, the average power consumption in the capsule could be maintained below the 100 mW safety limit previously reported for USCE devices [13].

Based on the silicon area and power limitations, the most attractive approach is to use an application-specific integrated circuit (ASIC) that incorporates most of the Tx and sensing functionality within a single, custom-made chip. In addition to the electronics design, this brings the need for complementary adjustments to conventional imaging protocols to reduce power consumption and mitigate peak currents.

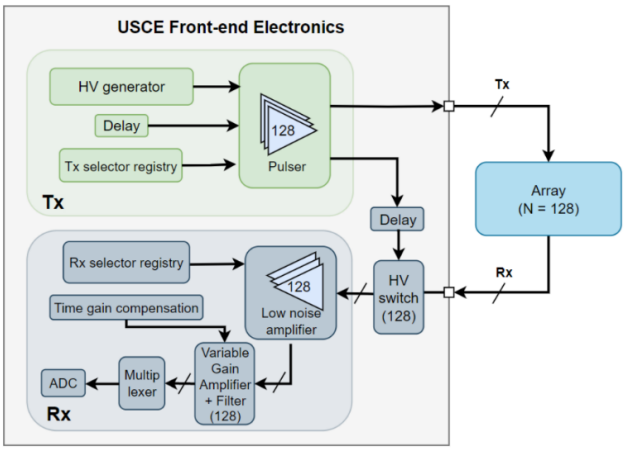

Fig. 2. Block diagram of the constitutive electronics of an USCE device

B. US Imaging for USCE

Conventionally, US B-mode images are acquired line by line (A-scans) sequentially. However, this lacks focusing capabilities, resulting in poor spatial resolution, and suffers from low signal-to-noise-ratio (SNR) when only one Tx element is used per A-scan due to the spreading of the unfocused acoustic wave and low Tx energy [14]. Moreover, SNR is proportional to the driving voltage of the array. However, voltages above 30V are difficult to supply within an USCE device because large amplification from a low voltage supply, such as the battery or WPT receiver, leads to low conversion efficiency in fully integrated applications with restricted space such as in USCE.

Techniques that improve the scan quality include beamforming on Tx through element phasing [15] and post-focusing techniques applied to the recorded echoes such as synthetic aperture (SA) [14]. Beamforming on Tx improves the lateral resolution of the scan and SNR by using multiple Tx elements for each Tx-Rx cycle and by focusing the US in a region of interest. However, it requires an individually addressable pulser and delay line for each element, leading to increased instantaneous power demands and chip footprint. In SA imaging, a Tx element or small group of Tx elements is excited, while all Rx elements are used to record the echo data. Then the next Tx element or small group is excited, and this continues until the full array aperture has been used. The data is then post-processed to focus the US beam sequentially at each point in the B-scan, leading to improved lateral resolution. This method requires a group or the same number of ADCs as Rx channels and cannot be implemented in USCE due to the power and space limitations discussed beforehand.

To maintain satisfactory SNR and lateral resolution, several steps can be followed in the design of electronics for USCE keeping in mind the above considerations. Firstly, SNR can be improved by transmitting on groups of elements, though at a cost of reduced lateral resolution because of the increased Tx aperture size. However, resolution can be improved by transmitting a spherical wave via time-delay

defocusing applied to the Tx elements [14]. Secondly, SA imaging can be implemented even with only one Rx channel active at any given time by stacking up A-scans recorded successively, but at a cost of reduced frame rate. This implementation requires sequential triggering and sequential acquisition, leading to N^2 A-scans required to form one B-scan, where N is the number of Rx channels. The resulting imaging frame rate can be calculated with the following equation:

$$f = c / (2*d*N^2) \quad (1)$$

where c is the speed of sound in the tissue and d is the maximum imaging depth.

IV. METHODOLOGY

The chosen 128-element, 28 MHz µUS array was driven with a bespoke CMOS pulser whose details were published previously [16]. Different Tx apertures were tested for the power measurements, comprising 1, 3, 5, 7, 11, 15, 64 and 128 array elements in parallel. The driving voltage was provided to the pulser using a precision source measurement unit (SMU, B29-1B, Keysight, CA, USA) and was set to 20 $V_{p\text{-}p}$, which was towards the upper operational limit for the circuit. Considering a maximum power supply of 75 mW from the WPT receiver, the target current limit from the onboard power supply was 3.75 mA.

The pulser was set to transmit a 17 ns pulse at a pulse repetition frequency (PRF) of 500 Hz, to allow the SMU to perform accurate i_{avg} measurements. Considering that N^2 A-scans are required to form an image, the resulting frame rate was too low for medical US imaging applications. However, data published in [17] shows that i_{avg} varies linearly with PRF, which allows estimation of the respective i_{avg} at the higher PRF values suitable for USCE. Therefore, considering a maximum imaging depth of ~10 mm to scan the intestinal wall, the desired PRF was estimated at 75 kHz, which resulted in a scaling factor (s) of 150 applicable to the measured i_{avg}. Furthermore, the average leakage current ($i_{leakage}$) consumed by the open-loaded pulser was recorded with the SMU and subtracted from the total driving current. Therefore, the average current consumed by the array elements at the required PRF could be determined from the current measured with the SMU with the following equation:

$$i_{avg} = s*i_{SMU} - i_{leakage} \quad (2)$$

where $s = PRF_{USCE} / PRF_{SMU\ measurement}$.

The instantaneous current (i) consumed by the array elements was measured with a P6022 current probe (Tektronix, Inc., Beaverton, OR, United States) placed on the wire supplying the transducers with the driving signal. The instantaneous voltage (v) was measured with a voltage probe at the array connector. The peak values of the current (i_{peak}) and voltage (V_{peak}) were then extracted from the v and i traces. For this measurement, the pulser output was compared with the output from one channel of a Verasonics Vantage HF 128, configured to operate with the same driving voltage of 20 $V_{p\text{-}p}$ and 10 mm imaging depth.

V. RESULTS

The average leakage current consumed by the open-loaded pulser measured with the SMU was ~2.0 µA. The value was constant for 250 Hz ⩽ PRF ⩽ 2000 Hz, indicating that it did not vary with the pulse repetition frequency of the transmitted waveform.

Fig. 3. (a) shows that i_{avg} increased with the number of Tx elements connected in parallel, but its value remained well below the available current supply limit set beforehand for all tested conditions. The peak current, Fig. 3. (b), exceeded the supply limit for any number of elements in the Tx aperture, but the pulse duration was very short (<50 ns). The increase in the current drawn led to a decrease in the driving voltage below the set level for both the pulser and the Verasonics, Fig. 3. (c) when more than 7 Tx elements were connected in parallel.

Finally, considering (1), the achievable frame rate for SA acquisition with 128 array elements was calculated to be 4.6 Hz for an imaging depth of 10 mm, well within the limits considered viable. If necessary, however, the frame rate could be increased up to 585 Hz if conventional line-by-line acquisition is used.

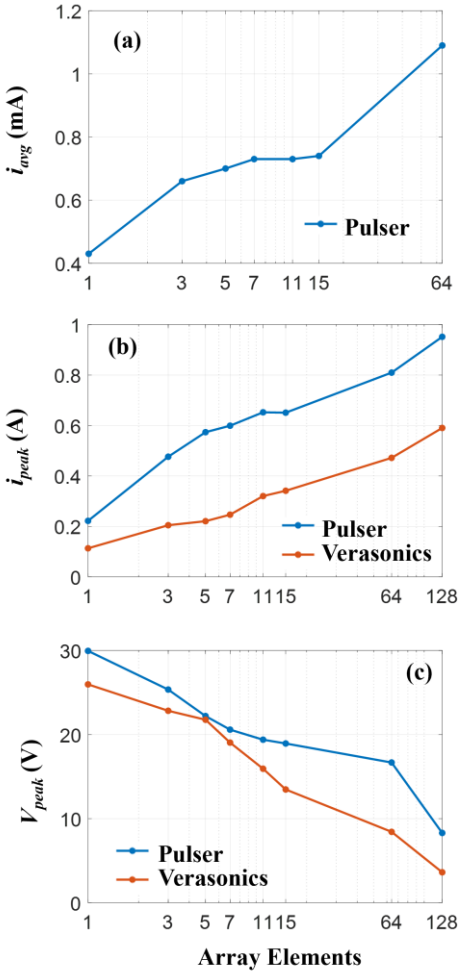

Fig. 3. Average current (a), peak current (b), and peak voltage (c) as function of the number or array elements connected in parallel.

VI. DISCUSSION

The increase in i_{avg} and i_{peak} did not follow a linear trend with the number of Tx elements connected in parallel because both the CMOS pulser and the Verasonics channel pulser could not supply the required current for more than 7 array elements resulting in a drop in the supply voltage

below the set value. The output power rating of a custom-made ASIC pulser could be further increased to sustain driving of a higher number of array elements but at the cost of larger size and higher power consumption, which might render the device unsuitable for USCE implementation.

V_{peak} was larger than the 20 V setting for Tx apertures < 7 elements because of the impedance mismatch between the pulser output impedance and the array impedance (~120 Ω for one array element and its connecting cable) and reflections in the connecting cables and associated connectors. This issue will be avoided in a fully integrated USCE device as all components are connected via short traces and no connectors are required.

i_{avg} was below the set current supply threshold for any number of Tx elements because of the low duty cycle of the transmitted waveform. This result, coupled with the high i_{peak} values measured for all evaluated conditions, strongly indicates that onboard power storage is required for USCE devices.

VII. CONCLUSIONS

USCE is a less painful and safer alternative to conventional endoscopy that benefits from full reach inside the GIT. Video capsule endoscopes have been in medical use for more than 20 years, but ultrasound-equipped capsules have not yet emerged as commercial products because of the size limitations and power constraints associated with the small scale of the devices. With recent advancements in circuit design and array miniaturization, USCE development is now under way.

WPT can be an effective means to provide power for capsule electronics, but its output is limited by the allowable SAR for human use. With power transfer rates in excess of 300 mW in air reported in literature, the achievable power transferred through phantom tissue published in another study was ~75 mW to maintain the SAR within the limits.

In this paper, we have measured the average current consumed by various Tx aperture sizes using a 128 element, 28 MHz μUS array and shown that its value was lower than the limit set by WPT for any number of Tx elements excited in parallel. However, the peak current consumed by the array elements was above the set limit, indicating that the USCE device must be equipped with onboard charge storage to sustain the pulser circuit during Tx. Furthermore, apertures < 7 array elements in parallel were shown to be the most suitable to be driven with a single pulser. For reception of ultrasonic data, space and power limitations restrict the number of Rx channels to one. SA can be implemented to increase the lateral resolution of the scan, but the ideal frame rate is reduced to 4.6 Hz as opposed to the much higher figure of 585 Hz for traditional line-by-line acquisition. Finally, the use of commercial off-the-shelf components should be reduced to a minimum as they occupy relatively large space, they are not optimized for USCE applications, and interconnecting them with other electronics can lead to noise and an increase in power consumption.

Future work will focus on imaging phantoms and ex-vivo tissue using the proposed protocols to determine the combination of Tx elements and post-focusing methods that maximize SNR and lateral resolution. The array will then be incorporated into a tethered probe for *in-vivo* evaluation.

REFERENCES

[1] Y. Qiu et al., "Ultrasound Capsule Endoscopy With a Mechanically Scanning Micro-ultrasound: A Porcine Study," Ultrasound in Medicine & Biology, vol. 46, no. 3, pp. 796–804, Mar. 2020, doi: 10.1016/j.ultrasmedbio.2019.12.003.

[2] X.-O. Qiu et al., "A New Ultrasound Capsule Endoscopy for Superficial and Submucosal Imaging of Esophagus: the first-in-human study," Gastrointestinal Endoscopy, vol. 0, no. 0, Jun. 2023, doi: 10.1016/j.gie.2023.06.015.

[3] P. Valdastri, M. Simi, and R. J. Webster, "Advanced Technologies for Gastrointestinal Endoscopy," Annual Review of Biomedical Engineering, vol. 14, no. 1, pp. 397–429, 2012, doi: 10.1146/annurev-bioeng-071811-150006.

[4] G. Iddan, G. Meron, A. Glukhovsky, and P. Swain, "Wireless capsule endoscopy," Nature, vol. 405, no. 6785, p. 417, May 2000, doi: 10.1038/35013140.

[5] X. Wang et al., "Development of a Mechanical Scanning Device With High-Frequency Ultrasound Transducer for Ultrasonic Capsule Endoscopy," IEEE Transactions on Medical Imaging, vol. 36, no. 9, pp. 1922–1929, Sep. 2017, doi: 10.1109/TMI.2017.2699973.

[6] J. H. Lee, G. Traverso, D. Ibarra-Zarate, D. S. Boning, and B. W. Anthony, "Ex Vivo and In Vivo Imaging Study of Ultrasound Capsule Endoscopy," J Med Device, vol. 14, no. 2, p. 021005, Jun. 2020, doi: 10.1115/1.4046352.

[7] J. M. Rothberg et al., "Ultrasound-on-chip platform for medical imaging, analysis, and collective intelligence," Proc. Natl. Acad. Sci. U.S.A., vol. 118, no. 27, p. e2019339118, Jul. 2021, doi: 10.1073/pnas.2019339118.

[8] R. Puers, R. Carta, and J. Thoné, "Wireless power and data transmission strategies for next-generation capsule endoscopes," J. Micromech. Microeng., vol. 21, no. 5, p. 054008, Apr. 2011, doi: 10.1088/0960-1317/21/5/054008.

[9] S. H. Kim and H. J. Chun, "Capsule Endoscopy: Pitfalls and Approaches to Overcome," Diagnostics, vol. 11, no. 10, p. 1765, Sep. 2021, doi: 10.3390/diagnostics11101765.

[10] S. R. Khan and M. P. Y. Desmulliez, "Towards a Miniaturized 3D Receiver WPT System for Capsule Endoscopy," Micromachines, vol. 10, no. 8, Art. no. 8, Aug. 2019, doi: 10.3390/mi10080545.

[11] M. Lin et al., "A fully integrated wearable ultrasound system to monitor deep tissues in moving subjects," Nat Biotechnol, May 2023, doi: 10.1038/s41587-023-01800-0.

[12] Boris Murmann, "ADC Performance Survey 1997-2022." https://web.stanford.edu/~murmann/adcsurvey.html (accessed Dec. 23, 2022).

[13] H. S. Lay et al., "In-Vivo Evaluation of Microultrasound and Thermometric Capsule Endoscopes," IEEE Transactions on Biomedical Engineering, vol. 66, no. 3, pp. 632–639, 2019, doi: 10.1109/TBME.2018.2852715.

[14] J. A. Jensen, S. I. Nikolov, K. L. Gammelmark, and M. H. Pedersen, "Synthetic aperture ultrasound imaging," Ultrasonics, vol. 44, pp. e5–e15, Dec. 2006, doi: 10.1016/j.ultras.2006.07.017.

[15] O. T. Von Ramm and S. W. Smith, "Beam Steering with Linear Arrays," IEEE Transactions on Biomedical Engineering, vol. BME-30, no. 8, pp. 438–452, Aug. 1983, doi: 10.1109/TBME.1983.325149.

[16] B. Abaravičius, A. Moldovan, S. Mitra, and S. Cochran, "Towards Integrated Microultrasound Systems," in 2022 IEEE International Ultrasonics Symposium (IUS), Oct. 2022, pp. 1–4. doi: 10.1109/IUS54386.2022.9957864.

[17] B. Abaravicius, A. Moldovan, S. Cochran, and S. Mitra, "Development of a Point-of-Care Ultrasound Driver for Applications with Low Power and Reduced Area Requirements," in 2021 IEEE International Ultrasonics Symposium (IUS), Sep. 2021, pp. 1–4. doi: 10.1109/IUS52206.2021.9593342.